A survey of super-heavy elements from a theoretical perspective

P.–G. Reinhard[1], J. Erler[2], P. Klüpfel[3], K.-H. Langanke[5], H.-P. Löns[5], G. Martinez-Pinedo[5], J.A. Maruhn[4].

[1] Institut für Theoretische Physik, Friedrich-Alexander-Universität, Erlangen/Germany

[2] Physics Division, Oak Ridge National Laboratory, Oak Ridge/USA

[3] Science Institute, University of Iceland, Dunhaga 3, IS-107 Reykjavik, Iceland

[4] Institut für Theoretische Physik, Johann-Wofgang-Goethe Universität, Frankfurt/Germany

[5] Gesellschaft für Schwerionenforschung, Darmstadt/Germany

Supported by the BMBF (contracts 06ER9063 & 06FY9086)

Outline

The Skyrme energy functional and its performance

The Skyrme energy functional

$$E_{\text{tot}} = E_{\text{kin}} + \int d^3r\, \mathcal{E}_{\text{Skyrme}}(\rho, \tilde{\rho}, \tau, \tilde{\tau}, \mathbf{J}, \tilde{\mathbf{J}}, \ldots) + \int d^3r\, \mathcal{E}_{\text{pair}}(\chi_p, \chi_n, \rho) + E_{\text{Coul}} - E_{\text{corr}}$$

The Skyrme energy functional

$$E_{\rm tot} = E_{\rm kin} + \int d^3r\, \mathcal{E}_{\rm Skyrme}(\rho, \tilde{\rho}, \tau, \tilde{\tau}, \mathbf{J}, \tilde{\mathbf{J}}, \ldots) + \int d^3r\, \mathcal{E}_{\rm pair}(\chi_p, \chi_n, \rho) + E_{\rm Coul} - E_{\rm corr}$$

- kinetic energy ($E_{\rm kin}$)
- effective potential energy ($\mathcal{E}_{\rm Skyrme}$)
- pairing functional ($\mathcal{E}_{\rm pair}$)
- Coulomb en. (exchange = Slater appr.) ($E_{\rm Coul}$)
- correlations from low energy modes: c.m., rotation, vibrat. ($E_{\rm corr}$)

The Skyrme energy functional

$$E_{\mathrm{tot}} = E_{\mathrm{kin}} + \int d^3r\, \mathcal{E}_{\mathrm{Skyrme}}(\rho, \tilde{\rho}, \tau, \tilde{\tau}, \mathbf{J}, \tilde{\mathbf{J}}, \ldots) + \int d^3r\, \mathcal{E}_{\mathrm{pair}}(\chi_p, \chi_n, \rho) + E_{\mathrm{Coul}} - E_{\mathrm{corr}}$$

kinetic energy

effective potential energy

pairing functional

Coulomb en. (exchange = Slater appr.)

correlations from low energy modes: c.m., rotation, vibrat.

functional of local densities and currents:

density	$\rho(r) = \sum_\alpha v_\alpha^2 \lvert\varphi_\alpha\rvert^2$
kinetic density	$\tau(r) = \sum_\alpha v_\alpha^2 \lvert\nabla\varphi_\alpha\rvert^2$
spin-orbit density	$\mathbf{J}(r) = -\mathrm{i}\sum_\alpha v_\alpha^2 \varphi_\alpha^\dagger \nabla\times\boldsymbol{\sigma}\varphi_\alpha$
spin density	$\boldsymbol{\sigma}(r) = \sum_\alpha v_\alpha^2 \varphi_\alpha^\dagger \hat{\boldsymbol{\sigma}}\varphi_\alpha$
current	$\mathbf{j}(r) = -\mathrm{i}\sum_\alpha v_\alpha^2 \varphi_\alpha^\dagger \nabla\varphi_\alpha + \mathrm{c.c.}$
spin-kinetic density	$\boldsymbol{\tau}(r) = -\mathrm{i}\sum_\alpha v_\alpha^2 \varphi_\alpha^\dagger \nabla\boldsymbol{\sigma}\nabla\varphi_\alpha$
total & difference	$\underbrace{\rho = \rho_n + \rho_p}_{\text{isoscalar}},\ \underbrace{\tilde{\rho} = \rho_n - \rho_p}_{\text{isovector}}$
pair density	$\chi(r) = \sum_\alpha u_\alpha v_\alpha \lvert\varphi_\alpha\rvert^2$
pairing amplit.	u_α, v_α

The Skyrme energy functional

$$E_{\rm tot} = E_{\rm kin} + \int d^3r\, \mathcal{E}_{\rm Skyrme}(\rho, \tilde{\rho}, \tau, \tilde{\tau}, \mathbf{J}, \tilde{\mathbf{J}}, \ldots) + \int d^3r\, \mathcal{E}_{\rm pair}(\chi_p, \chi_n, \rho) + E_{\rm Coul} - E_{\rm corr}$$

kinetic energy

effective potential energy

pairing functional

Coulomb en. (exchange = Slater appr.)

correlations from low energy modes: c.m., rotation, vibrat.

functional of local densities and currents:

density	$\rho(r) = \sum_\alpha v_\alpha^2 \lvert\varphi_\alpha\rvert^2$
kinetic density	$\tau(r) = \sum_\alpha v_\alpha^2 \lvert\nabla\varphi_\alpha\rvert^2$
spin-orbit density	$\mathbf{J}(r) = -\mathrm{i}\sum_\alpha v_\alpha^2 \varphi_\alpha^\dagger \nabla\times\boldsymbol{\sigma}\varphi_\alpha$
spin density	$\boldsymbol{\sigma}(r) = \sum_\alpha v_\alpha^2 \varphi_\alpha^\dagger \hat{\boldsymbol{\sigma}}\varphi_\alpha$
current	$\mathbf{j}(r) = -\mathrm{i}\sum_\alpha v_\alpha^2 \varphi_\alpha^\dagger \nabla\varphi_\alpha +$ c.c.
spin-kinetic density	$\boldsymbol{\tau}(r) = -\mathrm{i}\sum_\alpha v_\alpha^2 \varphi_\alpha^\dagger \nabla\boldsymbol{\sigma}\nabla\varphi_\alpha$
total & difference	$\underbrace{\rho = \rho_n + \rho_p}_{\text{isoscalar}},\ \underbrace{\tilde{\rho} = \rho_n - \rho_p}_{\text{isovector}}$
pair density	$\chi(r) = \sum_\alpha u_\alpha v_\alpha \lvert\varphi_\alpha\rvert^2$
pairing amplit.	u_α, v_α

mean-field equations: variation s.p. wave functions φ_α^*
variation of occupation amplitudes u_α

... and its parameterization

$$E_{\text{tot}} = E_{\text{kin}} + \int d^3r\, \mathcal{E}_{\text{Skyrme}}(\rho, \tilde{\rho}, \tau, \tilde{\tau}, \mathbf{J}, \tilde{\mathbf{J}}, \ldots) + \int d^3r\, \mathcal{E}_{\text{pair}}(\chi_p, \chi_n, \rho) + E_{\text{Coul}} - E_{\text{corr}}$$

... and its parameterization

$$E_{\text{tot}} = E_{\text{kin}} + \int d^3r\, \mathcal{E}_{\text{Skyrme}}(\rho, \tilde{\rho}, \tau, \tilde{\tau}, \mathbf{J}, \tilde{\mathbf{J}}, \ldots) + \int d^3r\, \mathcal{E}_{\text{pair}}(\chi_p, \chi_n, \rho) + E_{\text{Coul}} - E_{\text{corr}}$$

The Skyrme energy functional can be quantified in terms of the following parameters:

$\underline{\mathcal{E}_{\text{Skyrme}}}$:

		isoscalar		*isovector*
bulk:	bulk equilibrium	E/A, $\rho_{0,equil}$		
	incompressibility	K	, symmetry energy	a_{sym}
	surface energy	a_{surf}	, surf.symm. energy	$a_{\text{surf,sym}}$
	effective mass	m^*/m	, TRK sum rule	κ_{TRK}
s.p.:	spin-orbit	b_4	, isovect. spin orbit	b'_4

$\underline{\mathcal{E}_{\text{pair}}}$:

proton and neutron pairing strenghts: $V_{\text{pair},p}$, $V_{\text{pair},n}$

... and its parameterization

$$E_{\rm tot} = E_{\rm kin} + \int d^3r\, \mathcal{E}_{\rm Skyrme}(\rho, \tilde{\rho}, \tau, \tilde{\tau}, \mathbf{J}, \tilde{\mathbf{J}}, ...) + \int d^3r\, \mathcal{E}_{\rm pair}(\chi_p, \chi_n, \rho) + E_{\rm Coul} - E_{\rm corr}$$

The Skyrme energy functional can be quantified in terms of the following parameters:

$\mathcal{E}_{\rm Skyrme}$:

		isoscalar		*isovector*
bulk:	bulk equilibrium	E/A, $\rho_{0,equil}$		
	incompressibility	K	, symmetry energy	$a_{\rm sym}$
	surface energy	$a_{\rm surf}$	, surf.symm. energy	$a_{\rm surf,sym}$
	effective mass	m^*/m	, TRK sum rule	$\kappa_{\rm TRK}$
s.p.:	spin-orbit	b_4	, isovect. spin orbit	b'_4

$\mathcal{E}_{\rm pair}$:

proton and neutron pairing strenghts: $V_{{\rm pair},p}$, $V_{{\rm pair},n}$

The parameters are adjusted to empirical data (↔ least squares fits).

... and its parameterization

$$E_{\text{tot}} = E_{\text{kin}} + \int d^3r\,\mathcal{E}_{\text{Skyrme}}(\rho, \tilde{\rho}, \tau, \tilde{\tau}, \mathbf{J}, \tilde{\mathbf{J}}, \ldots) + \int d^3r\,\mathcal{E}_{\text{pair}}(\chi_p, \chi_n, \rho) + E_{\text{Coul}} - E_{\text{corr}}$$

The Skyrme energy functional can be quantified in terms of the following parameters:

$\mathcal{E}_{\text{Skyrme}}$:

		isoscalar		*isovector*
bulk:	bulk equilibrium	E/A, $\rho_{0,equil}$		
	incompressibility	K	, symmetry energy	$a_{\text{sym}} = 30\pm2$ MeV
	surface energy	a_{surf}	, surf.symm. energy	$a_{\text{surf,sym}}$
	effective mass	$m^*/m = 0.9\pm0.15$	, TRK sum rule	$\kappa_{\text{TRK}} = 0.1\pm0.4$
s.p.:	spin-orbit	b_4	, isovect. spin orbit	b_4'

$\mathcal{E}_{\text{pair}}$:

proton and neutron pairing strenghts: $V_{\text{pair},p}$, $V_{\text{pair},n}$

The parameters are adjusted to empirical data ($\leftrightarrow$ least squares fits).

Fit to ground state properties $\Longrightarrow$ fix parameters $\leftrightarrow$ parameterization **SV-min**

... and its parameterization

$$E_{\rm tot} = E_{\rm kin} + \int d^3r\,\mathcal{E}_{\rm Skyrme}(\rho,\tilde{\rho},\tau,\tilde{\tau},\mathbf{J},\tilde{\mathbf{J}},\ldots) + \int d^3r\,\mathcal{E}_{\rm pair}(\chi_p,\chi_n,\rho) + E_{\rm Coul} - E_{\rm corr}$$

The Skyrme energy functional can be quantified in terms of the following parameters:

$\mathcal{E}_{\rm Skyrme}$:

		isoscalar		isovector
bulk:	bulk equilibrium	E/A, $\rho_{0,equil}$		
	incompressibility	K	, symmetry energy	$a_{\rm sym} = 30$
	surface energy	$a_{\rm surf}$	, surf.symm. energy	$a_{\rm surf,sym}$
	effective mass	$m^*/m = 0.9$	, TRK sum rule	$\kappa_{\rm TRK} = 0.4$
s.p.:	spin-orbit	b_4	, isovect. spin orbit	b'_4

$\mathcal{E}_{\rm pair}$:

proton and neutron pairing strenghts: $V_{{\rm pair},p}$, $V_{{\rm pair},n}$

The parameters are adjusted to empirical data ($\leftrightarrow$ least squares fits).

Fit to ground state properties $\Longrightarrow$ fix parameters $\leftrightarrow$ parameterization **SV-min**

Info from giant resonance & neutron radius $\Longrightarrow$ fix also parameters $\leftrightarrow$ **SV-bas**

... and its parameterization

$$E_{\text{tot}} = E_{\text{kin}} + \int d^3r\,\mathcal{E}_{\text{Skyrme}}(\rho,\tilde{\rho},\tau,\tilde{\tau},\mathbf{J},\tilde{\mathbf{J}},...) + \int d^3r\,\mathcal{E}_{\text{pair}}(\chi_p,\chi_n,\rho) + E_{\text{Coul}} - E_{\text{corr}}$$

The Skyrme energy functional can be quantified in terms of the following parameters:

$\mathcal{E}_{\text{Skyrme}}$:

		isoscalar		isovector
bulk:	bulk equilibrium	E/A, $\rho_{0,equil}$		
	incompressibility	K	, symmetry energy	$a_{\text{sym}} = 30$
	surface energy	a_{surf}	, surf.symm. energy	$a_{\text{surf,sym}}$
	effective mass	$m^*/m = 0.9$	, TRK sum rule	$\kappa_{\text{TRK}} = 0.4$
s.p.:	spin-orbit	b_4	, isovect. spin orbit	b'_4

$\mathcal{E}_{\text{pair}}$:

proton and neutron pairing strenghts: $V_{\text{pair},p}$, $V_{\text{pair},n}$

The parameters are adjusted to empirical data ($\leftrightarrow$ least squares fits).

Fit to ground state properties $\Longrightarrow$ fix parameters ▭ $\leftrightarrow$ parameterization SV-min

Info from giant resonance & neutron radius $\Longrightarrow$ fix also parameters ▭ $\leftrightarrow$ SV-bas

$\Longrightarrow$: some aspects vaguely determined $\Longrightarrow$ some uncertainty in extrapolations

... and its parameterization

$$E_{\rm tot} = E_{\rm kin} + \int d^3r\,\mathcal{E}_{\rm Skyrme}(\rho,\tilde{\rho},\tau,\tilde{\tau},\mathbf{J},\tilde{\mathbf{J}},...) + \int d^3r\,\mathcal{E}_{\rm pair}(\chi_p,\chi_n,\rho) + E_{\rm Coul} - E_{\rm corr}$$

The Skyrme energy functional can be quantified in terms of the following parameters:

$\mathcal{E}_{\rm Skyrme}$:

		isoscalar		isovector
bulk:	bulk equilibrium	E/A, $\rho_{0,equil}$		
	incompressibility	K	, symmetry energy	$a_{\rm sym} = 30$
	surface energy	$a_{\rm surf}$	, surf.symm. energy	$a_{\rm surf,sym}$
	effective mass	$m^*/m = 0.9$	, TRK sum rule	$\kappa_{\rm TRK} = 0.4$
s.p.:	spin-orbit	b_4	, isovect. spin orbit	b'_4

$\mathcal{E}_{\rm pair}$:

proton and neutron pairing strenghts: $V_{{\rm pair},p}$, $V_{{\rm pair},n}$

The parameters are adjusted to empirical data ($\leftrightarrow$ least squares fits).

Fit to ground state properties $\Longrightarrow$ fix parameters $\leftrightarrow$ parameterization SV-min

Info from giant resonance & neutron radius $\Longrightarrow$ fix also parameters $\leftrightarrow$ SV-bas

$\Longrightarrow$: some aspects vaguely determined $\Longrightarrow$ some *freedom* in extrapolations

Shell gap and magic numbers

Seperation energies, halting points and shell gaps

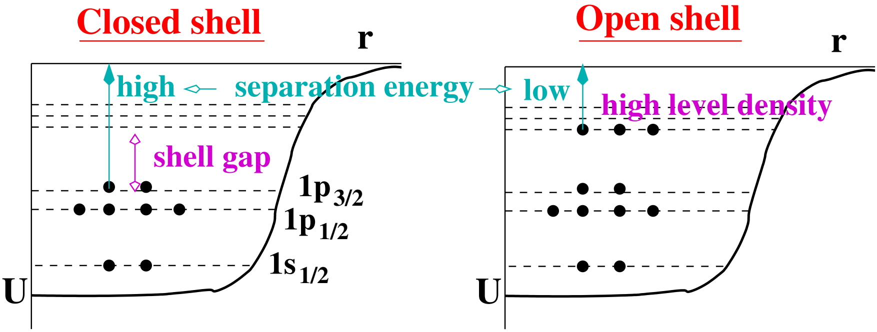

(example: nuclear potential, harmonic osc. labelling, l*s)

- large separation energy (S_{2n}, S_{2p})
- enhanced binding ("shell correction") $\Longrightarrow$ high abundance
- enhanced fission stability

- low separation energy (S_{2n}, S_{2p})
- reduced prob. in evaporation chains (e.g. r-process)
- less stable against fission

Well developed shell gaps – example ^{208}Pb

single nucleon spectra near the Fermi energy for ^{208}Pb for a variety of models

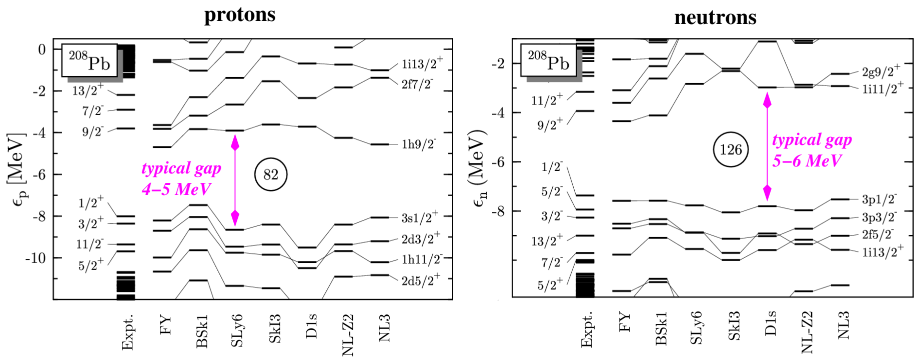

proton and neutron shell gaps are well developed for all models and forces

$\Longrightarrow$ the “magic numbers” $Z = 82$ and $N = 126$ well visible

Single nucleon spectra and shell gaps in SHE

single nucleon spectra near the Fermi energy for SHE Z=114/N=184
computed for a variety of mean-field models

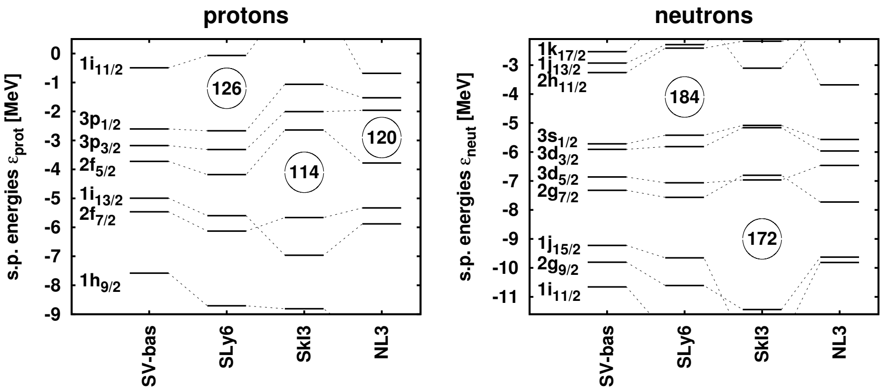

spectrum much more diffuse than in ^{208}Pb

Single nucleon spectra and shell gaps in SHE

single nucleon spectra near the Fermi energy for SHE Z=114/N=184
computed for a variety of mean-field models
plotted with multiplicity of states to indicate density of states (d.o.s)

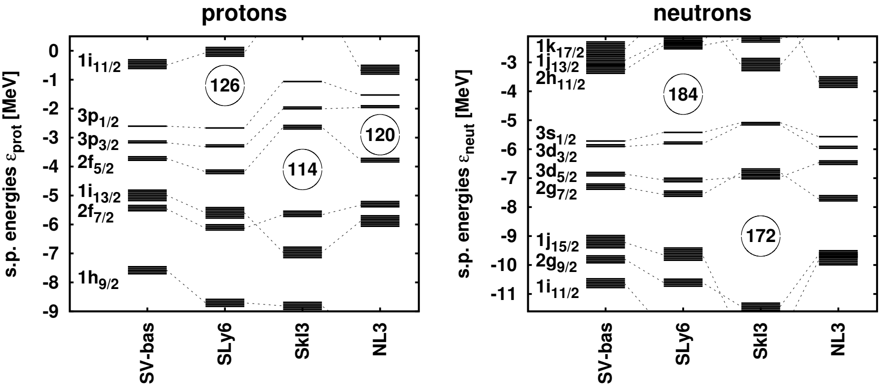

Single nucleon spectra and shell gaps in SHE

single nucleon spectra near the Fermi energy for SHE Z=114/N=184
computed for a variety of mean-field models
plotted with multiplicity of states to indicate density of states (d.o.s)

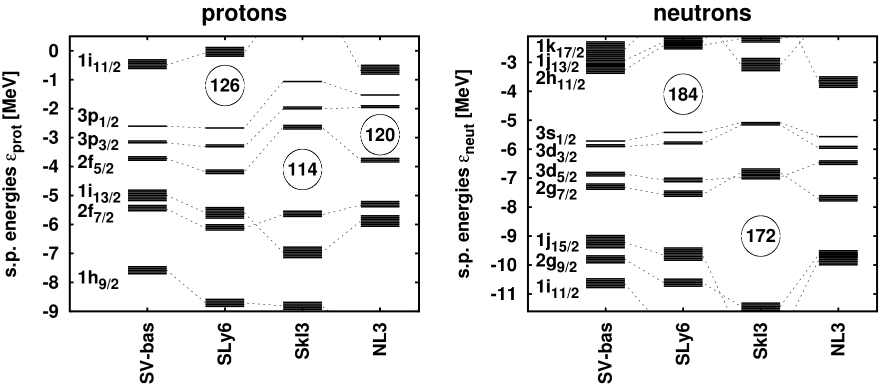

protons: high d.o.s. $Z \lesssim 114$ & $Z \gtrsim 126$, loosely filled $114 < Z < 126$
$\Longrightarrow$ floating & weak shell closures, broad region of shell stabilization

Two-nucleon shell gaps in SHE

Compute spectral shell gaps from two-nucleon energy differences:

$$\delta_{2n} = E(Z, N+2) - 2E(Z, N) + E(Z, N-2)$$
$$\delta_{2p} = E(Z+2, N) - 2E(Z, N) + E(Z-2, N)$$

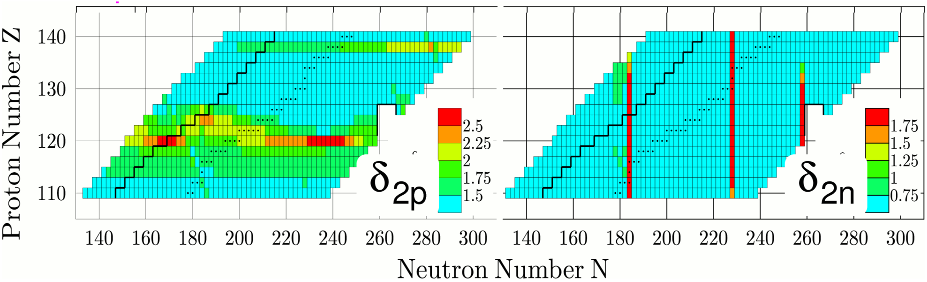

proton and neutron shell gaps are very weak $\longleftrightarrow$ $\Delta_{2N} \approx 2$ MeV
particularly for protons: broad regions of enhanced gaps

The softness of SHE ($Z \gtrapprox 114$)

intruders in "energy gap" $\longleftrightarrow$ soft potential-energy surface expected

The softness of SHE ($Z \gtrapprox 114$)

intruders in "energy gap" $\longleftrightarrow$ soft potential-energy surface expected

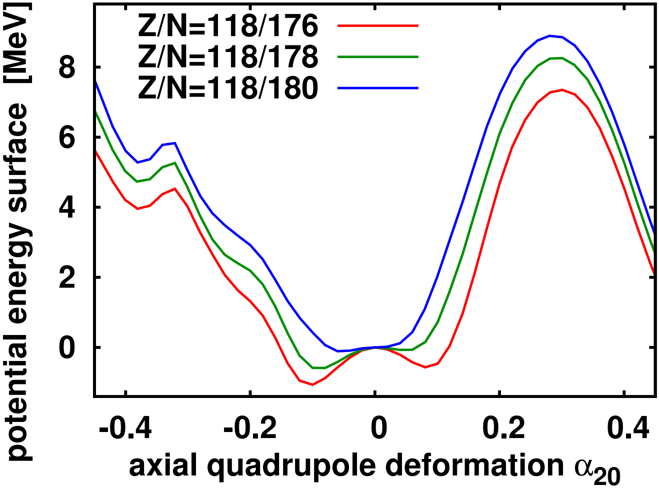

no clear minimum

rather broad region of comparable energies (often shape isomerism)

The softness of SHE ($Z \gtrapprox 114$)

intruders in “energy gap” $\longleftrightarrow$ soft potential-energy surface expected

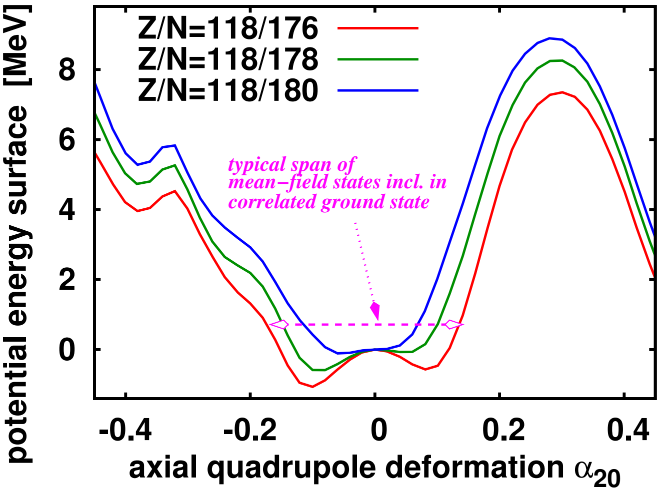

no clear minimum

rather broad region of comparable energies (often shape isomerism)

$\Longrightarrow$

correlated ground state

=

coherent superposition of diff. deformations

$|\Psi\rangle = \int \mathrm{d}\alpha_{20} |\Phi_{\alpha_{20}}\rangle f(\alpha_{20})$

Fission of SHE

Coulomb instability and shell stabilization

nuclear shapes along the fission path (schematic)

actual microscopic path $\{|\Phi_{\alpha_{20}}\rangle\}$
computed self-consistently
by constrained H.F.

$\Longrightarrow$

deformation energy surface $\mathcal{V}(\alpha_{20})$,

basis for collective description
of the fission dynamics

shell structure adds energy correction
$\Longrightarrow$ binding pocket $\leftrightarrow$ low d.o.s.
$\Longrightarrow$ fission barrier $\leftrightarrow$ high d.o.s.

Note: "shell correction" automatically
in self-consistent calculations

potential energy surface along fission path

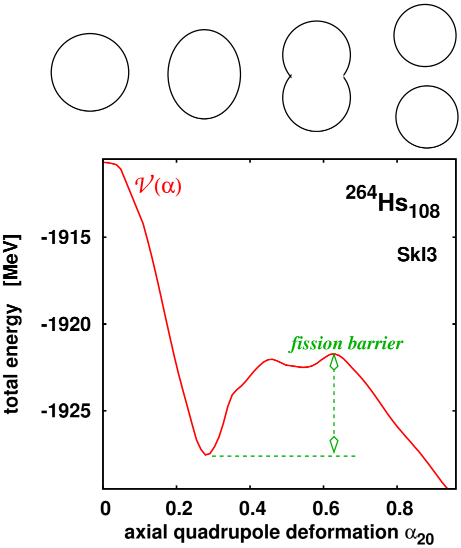

Different types of fission paths and their regimes

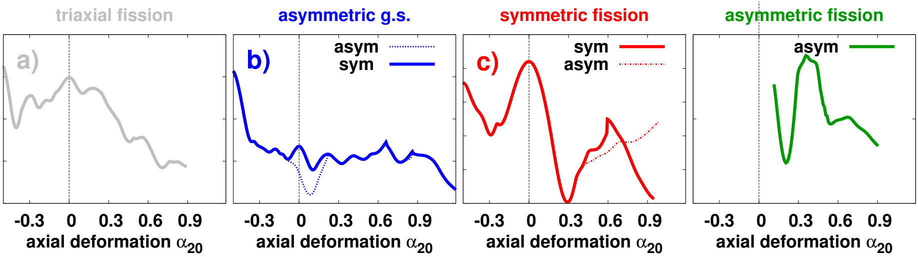

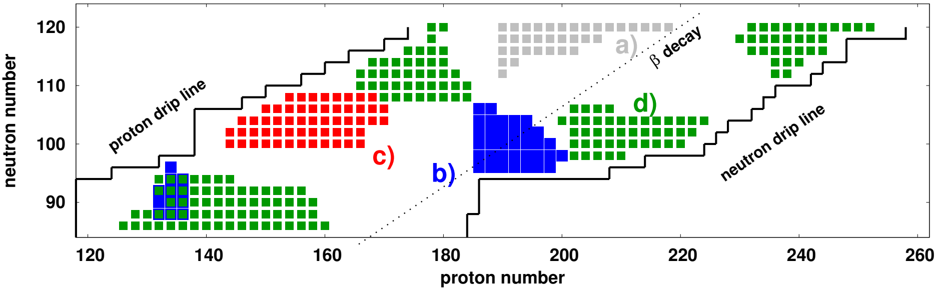

Systematics of barriers in SHE – for the parameterization SV-bas

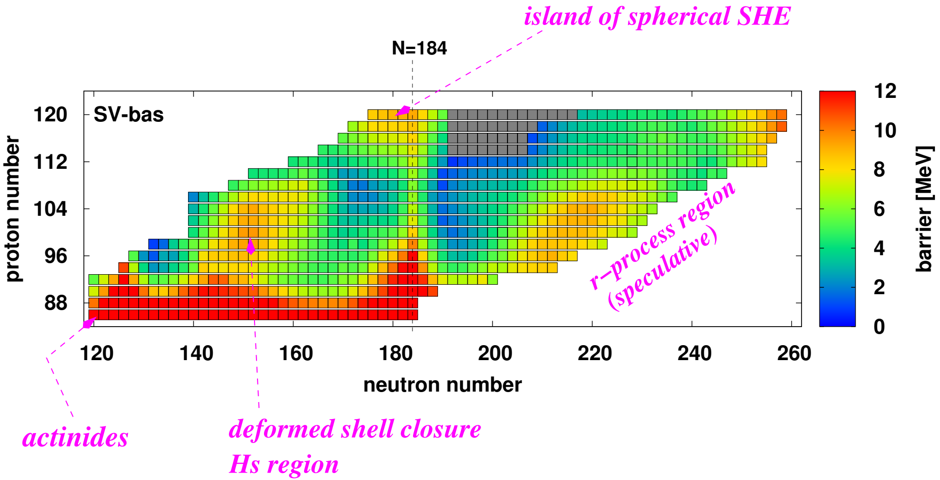

Systematics of barriers in SHE – for the parameterization SV-bas

broad regions of fission stability
(as anticipated by shell structure)

island of spherical SHE

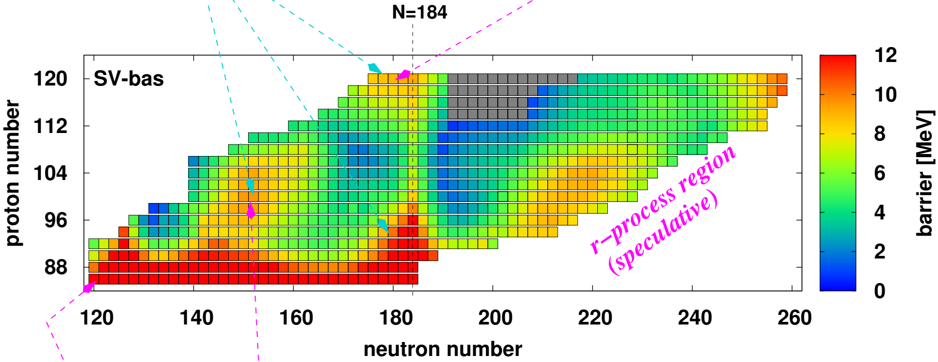

actinides

deformed shell closure
Hs region

Systematics of barriers in SHE – for the parameterization SV-bas

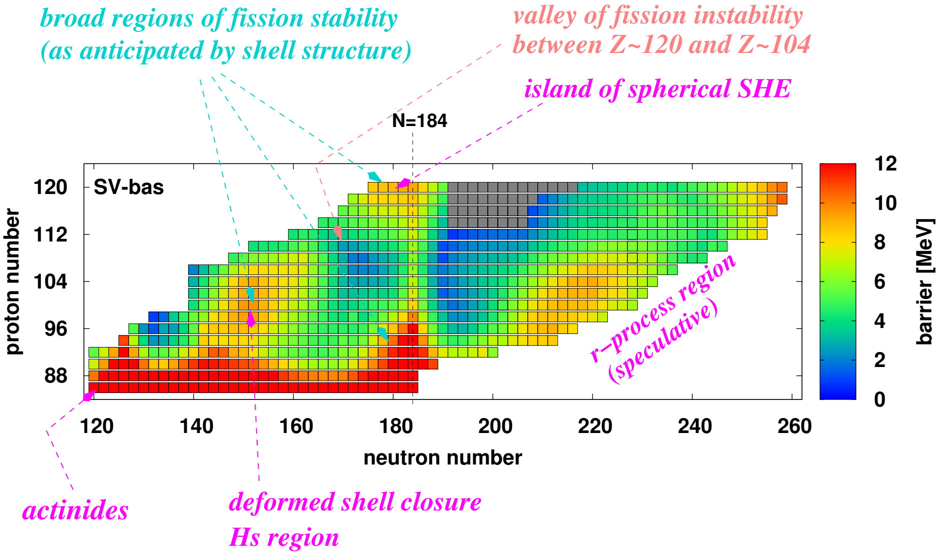

Systematics of barriers in SHE – several forces

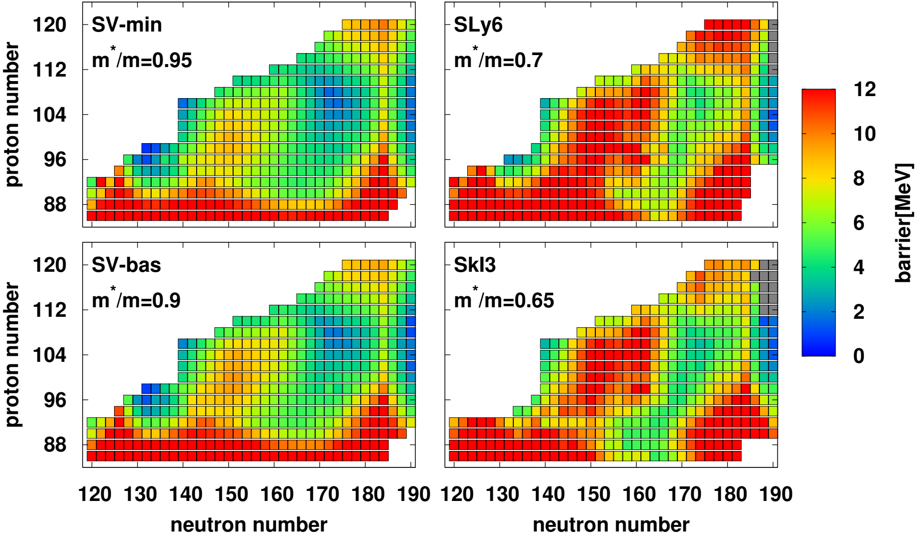

pattern similar for all forces – but barrier heights vary dramatically

barrier height ⟷ average d.o.s. ⟷ effective mass m^*/m

Computation of fission lifetimes

Computation of fission life-times

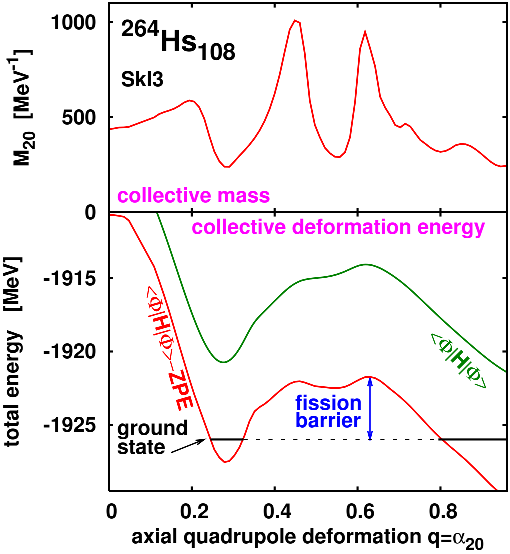

1) Deformation path $|\Phi_q\rangle$ (CHF):
$$\delta_{\langle\Phi_q|}\langle\Phi_q|\hat{H}-\lambda\hat{Q}_{20}|\Phi_q\rangle = 0$$
2) Deformation energy $\mathcal{V}$:
$$\mathcal{V}(q) = \langle\Phi_q|\hat{H}|\Phi_q\rangle$$
3) Collective mass $\mathcal{M}$ (lin.resp.):
$$[\hat{H},\hat{R}]|\Phi_q\rangle = \mathrm{i}\partial_q|\Phi_q\rangle$$
$$\mathcal{M}^{-1} = \langle\Phi_q|[\hat{R},[\hat{H},\hat{R}]]|\Phi_q\rangle$$
4) Momentum of inertia $\Theta \leftrightarrow$ as $\mathcal{M}$
5) Quantum corrected energy V:
$$V = \mathcal{V} - \mathcal{Z}_{\mathrm{vib}} - \mathcal{Z}_{\mathrm{rot}}$$
($\mathcal{Z} \equiv$ zero-point energy)
6) Ground state energy E_{gs}:
solve Schr.eq. with V and $\mathcal{M}$
7) Tunneling probability $P \leftrightarrow$ WKB
8) Repetition time $T_{\mathrm{rep}} \leftrightarrow$ WKB

$\Longrightarrow$ fission lifetime $\tau_{\mathrm{fis}} = T_{\mathrm{rep}}/P$

"ab initio" – no free parameters

Test fission lifetimes for transactinides

predictions vary sizeably

$\tau_{\rm fiss}$ depends on m^*/m

$m^*/m = 0.9 - 1$
$\Rightarrow$ reasonable results

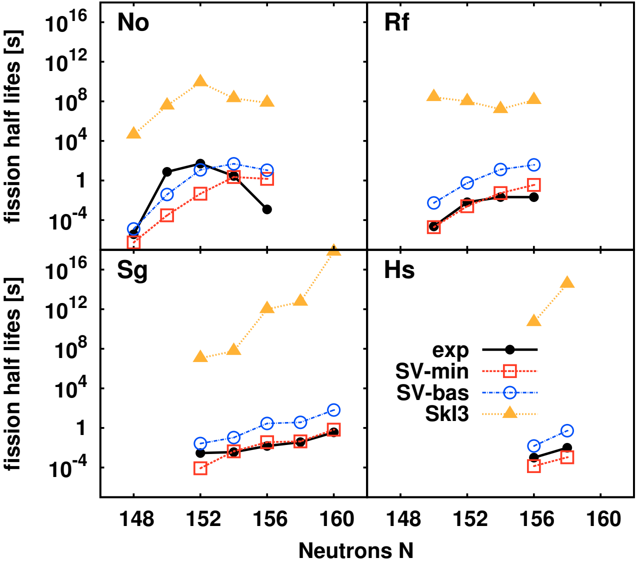

Test fission lifetimes for SHE

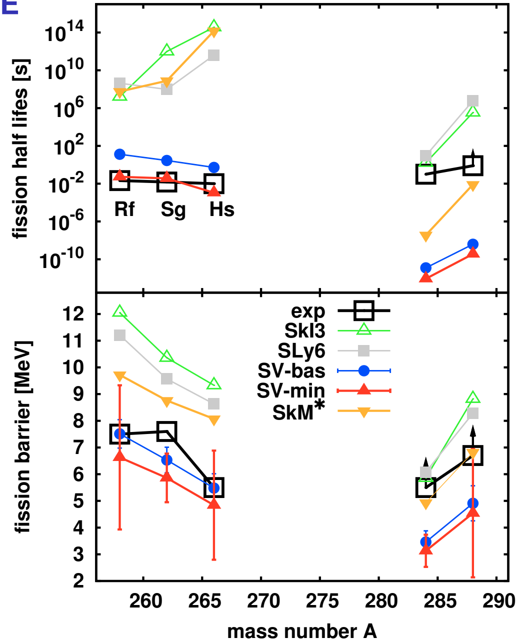

unresolved trend:

forces which perform very well for $Z \approx 100$

underestimate τ_{fiss} for $Z \approx 114$

and vice versa

Systematics of lifetimes for a variety of forces

valley of fission instability

SLy6 & SkI3 (low m/m ~ 0.6–0.7) overestimate fission stability*

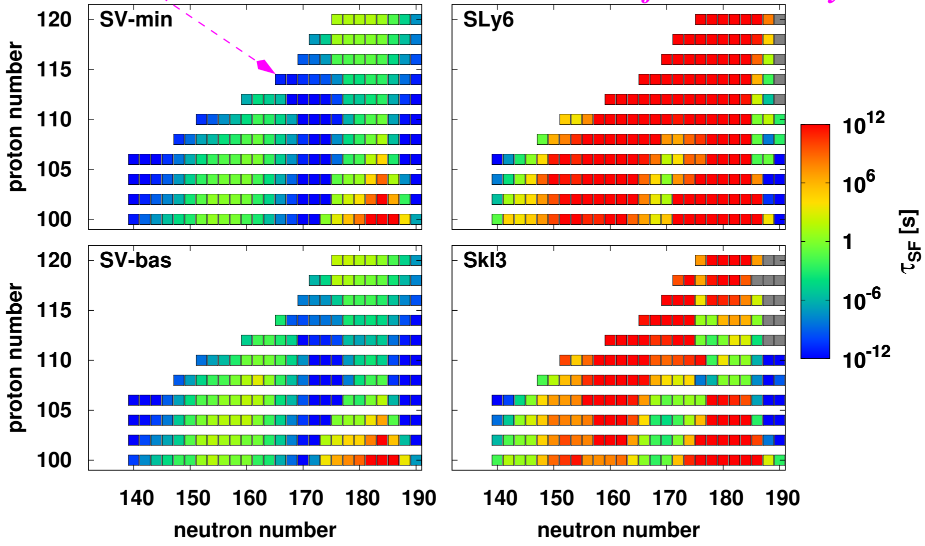

Competing channels: α- and β-decay

Test of α decay lifetimes

compute α-decay lifetimes τ_α from Q_α using Viola systematics

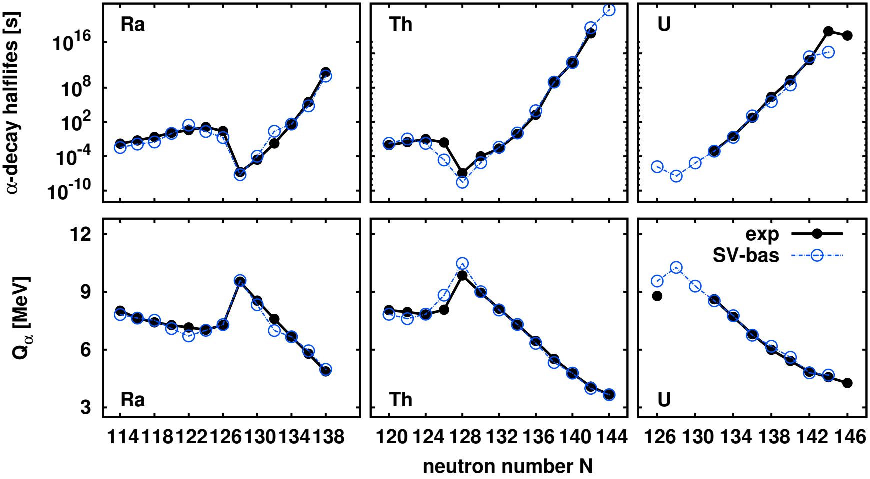

$\Longrightarrow$ recent Skyrme parameterizations describe α-decay in actinides very well

Test of α decay for SHE – correlation effects

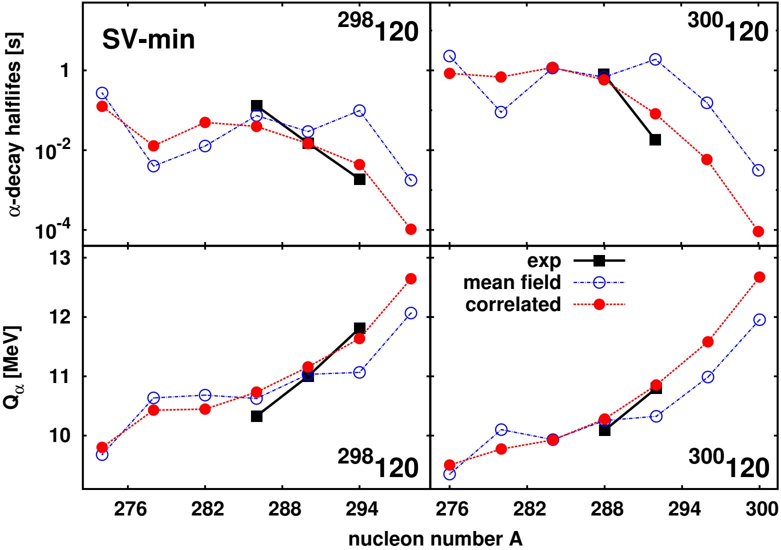

$\Longrightarrow$ 1) recent Skyrme parameterizations describe α-decay in SHE very well
2) ground-state correlations become important in SHE for a detailed description

Compare lifetimes: fission – α decay

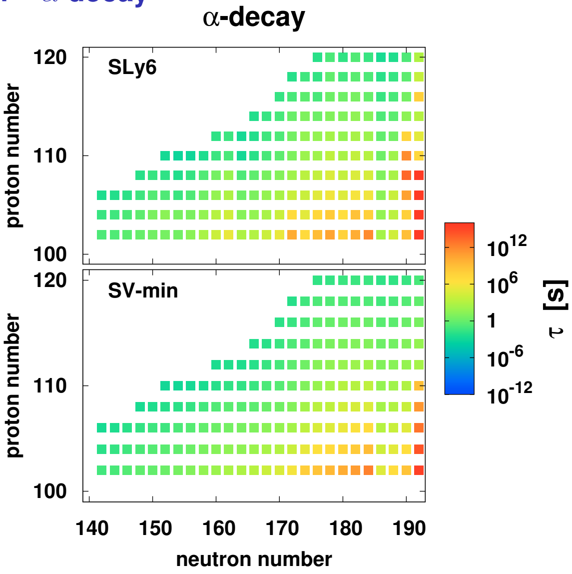

smoothly varying, independent of force

Compare lifetimes: fission – α decay

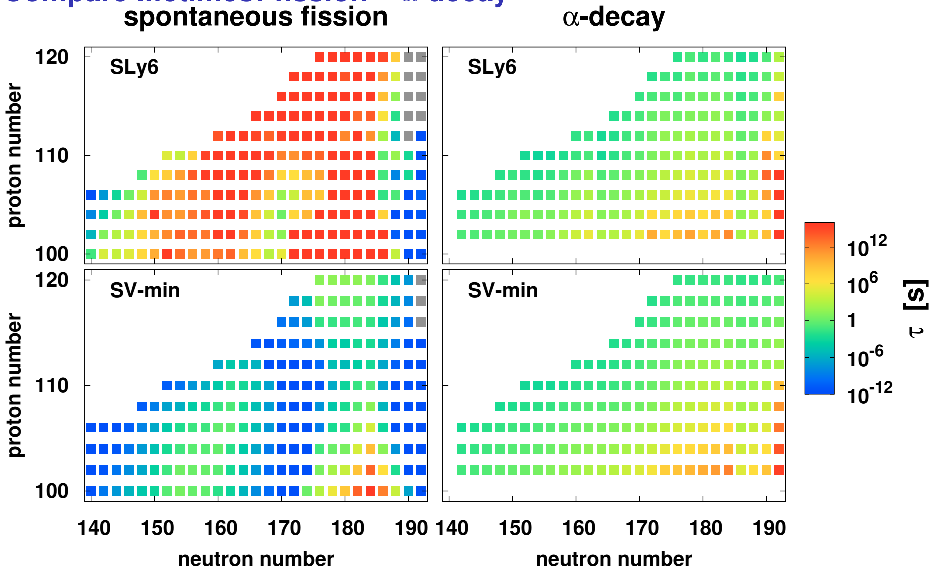

strong fluctuations, force dependent $\longleftrightarrow$ smoothly varying, independent of force

Compare lifetimes: fission – α decay – β decay

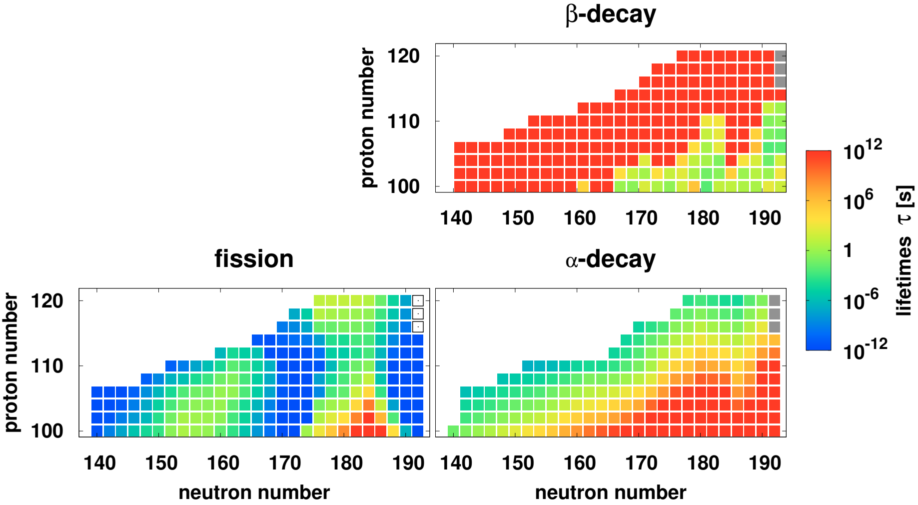

fission fluctuates strongly
pattern robust (shell structure)
magnitude depends on force

α- & β-decay lifetimes vary smoothly
and are rather independent of force

Dominant decay channel: fission – α decay – β decay

plot the decay mode
with shortest lifetime τ

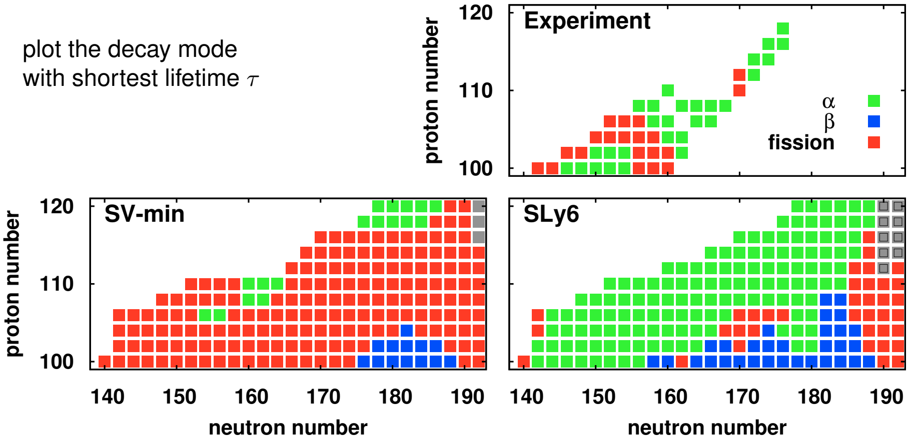

experimental trend roughly reproduced by SV-min – SLy6 yields too much fission stability

Conclusions

Fading away of magic numbers
broad band of low density of states $\leftrightarrow$ broad islands of shell stabilization
SHE $Z \gtrapprox 114$ are soft vibrators, may show pronounced shape isomerism

Conclusions

Fading away of magic numbers
broad band of low density of states $\leftrightarrow$ broad islands of shell stabilization
SHE $Z \gtrapprox 114$ are soft vibrators, may show pronounced shape isomerism

Robustness of shell structure
broad islands stabilization (Z/N$\approx$104/150 deformed, Z/N$\approx$116/172 spherical)
& fission valley in between

Conclusions

Fading away of magic numbers
broad band of low density of states $\leftrightarrow$ broad islands of shell stabilization
SHE $Z \gtrapprox 114$ are soft vibrators, may show pronounced shape isomerism

Robustness of shell structure
broad islands stabilization (Z/N≈104/150 deformed, Z/N≈116/172 spherical)
& fission valley in between

Different predictions for barrier heights and fission lifetimes
high m^*/m and/or high pairing $\leftrightarrow$ low barriers & τ_{fiss} $\leftrightarrow$ more realistic
low m^*/m and/or low pairing $\leftrightarrow$ high barriers & τ_{fiss}

Conclusions

Fading away of magic numbers
broad band of low density of states $\leftrightarrow$ broad islands of shell stabilization
SHE $Z \gtrapprox 114$ are soft vibrators, may show pronounced shape isomerism

Robustness of shell structure
broad islands stabilization (Z/N≈104/150 deformed, Z/N≈116/172 spherical)
& fission valley in between

Different predictions for barrier heights and fission lifetimes
high m^*/m and/or high pairing $\leftrightarrow$ low barriers & $\tau_{\rm fiss}$ $\leftrightarrow$ more realistic
low m^*/m and/or low pairing $\leftrightarrow$ high barriers & $\tau_{\rm fiss}$

Robustness of α- and β-decay lifetimes
Q_α, Q_β, τ_α, τ_β vary smoothly over landscape of SHE
well predicted by all reasonable Skyrme forces (= good ground state properties)

Conclusions

Fading away of magic numbers
broad band of low density of states $\leftrightarrow$ broad islands of shell stabilization
SHE $Z \gtrapprox 114$ are soft vibrators, may show pronounced shape isomerism

Robustness of shell structure
broad islands stabilization (Z/N≈104/150 deformed, Z/N≈116/172 spherical)
& fission valley in between

Different predictions for barrier heights and fission lifetimes
high m^*/m and/or high pairing $\leftrightarrow$ low barriers & $\tau_{\rm fiss}$ $\leftrightarrow$ more realistic
low m^*/m and/or low pairing $\leftrightarrow$ high barriers & $\tau_{\rm fiss}$

Robustness of α- and β-decay lifetimes
Q_α, Q_β, τ_α, τ_β vary smoothly over landscape of SHE
well predicted by all reasonable Skyrme forces (= good ground state properties)

Predictions of prevalent decay mode
works fine for most recent Skyrme models with $m^*/m \approx 0.9$ (SV-min, SV-bas)
improvements in detail still needed (need slightly larger $\tau_{\rm fiss}$ for $Z \geq 112$)

Conclusions

Fading away of magic numbers
broad band of low density of states $\leftrightarrow$ broad islands of shell stabilization
SHE $Z \gtrsim 114$ are soft vibrators, may show pronounced shape isomerism

Robustness of shell structure
broad islands stabilization (Z/N≈104/150 deformed, Z/N≈116/172 spherical)
& fission valley in between

Different predictions for barrier heights and fission lifetimes
high m^*/m and/or high pairing $\leftrightarrow$ low barriers & $\tau_{\rm fiss}$ $\leftrightarrow$ more realistic
low m^*/m and/or low pairing $\leftrightarrow$ high barriers & $\tau_{\rm fiss}$

Robustness of α- and β-decay lifetimes
Q_α, Q_β, τ_α, τ_β vary smoothly over landscape of SHE
well predicted by all reasonable Skyrme forces (= good ground state properties)

Predictions of prevalent decay mode
works fine for most recent Skyrme models with $m^*/m \approx 0.9$ (SV-min, SV-bas)
improvements in detail still needed (need slightly larger $\tau_{\rm fiss}$ for $Z \geq 112$)

Open problems
wrong trend of $\tau_{\rm fiss}$ from island Z=104 to island Z=116 (still for all Skyrme forces)

Experimental shell gaps

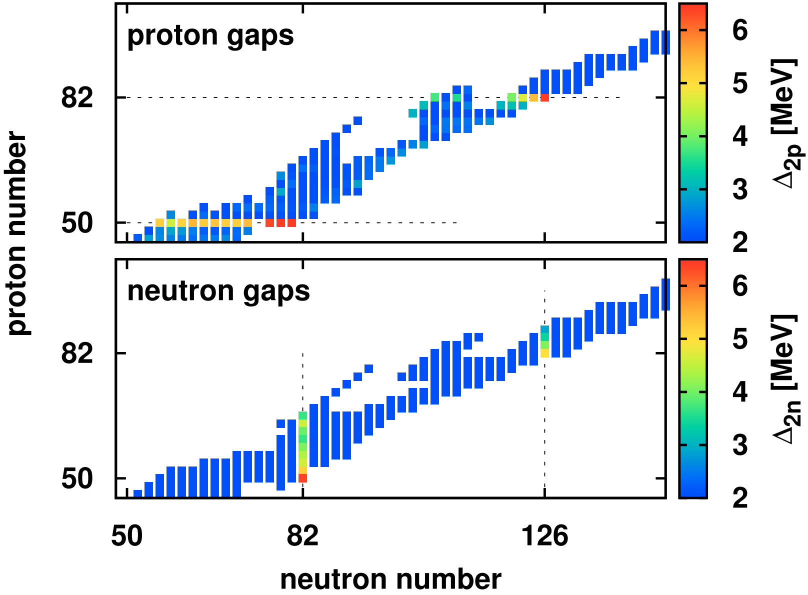

Test of performance for S_{2n}

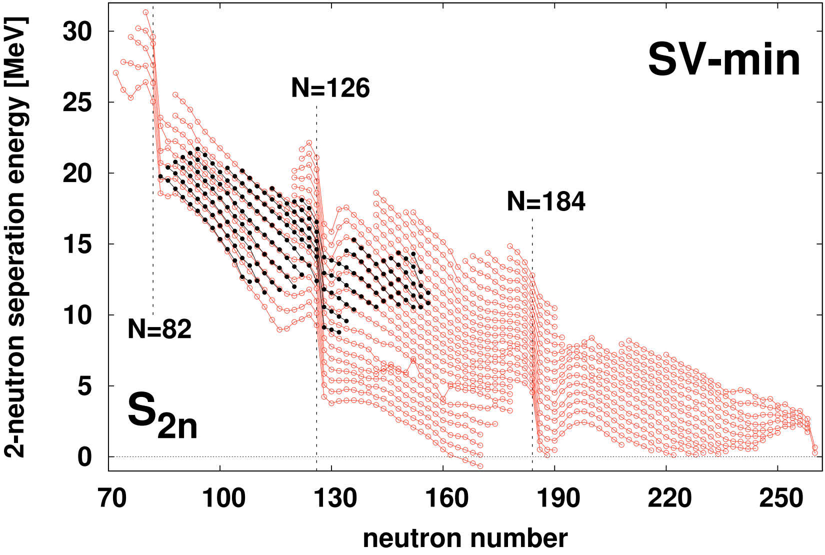

Coulomb instability and shell stabilization

nuclear shapes along the fission path (schematic)

actual microscopic path $\{|\Phi_{\alpha_{20}}\rangle\}$
computed self-consistently
by constrained H.F.

$\Longrightarrow$

deformation energy surface $\mathcal{V}(\alpha_{20})$,
basis for collective description
of the fission dynamics

potential energy surface along fission path

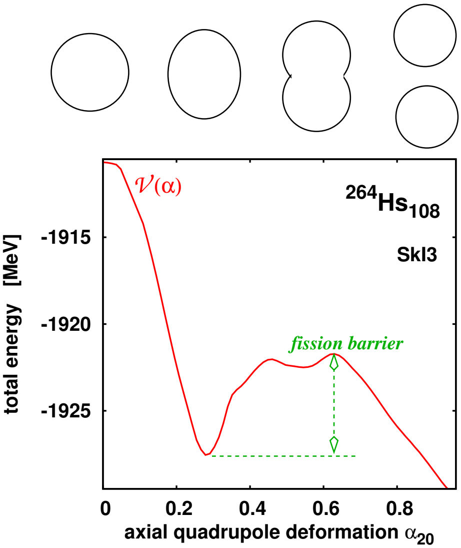

Coulomb instability and shell stabilization

density of state (d.o.s.)
at Fermi surface varies along path

^{264}Hs immediately fission unstable
in liquid drop model (LDM)

shell structure adds energy correction
$\Longrightarrow$ binding pocket $\leftrightarrow$ low d.o.s.
$\Longrightarrow$ fission barrier $\leftrightarrow$ high d.o.s.

Note: "shell correction" automatically
in self-consistent calculations

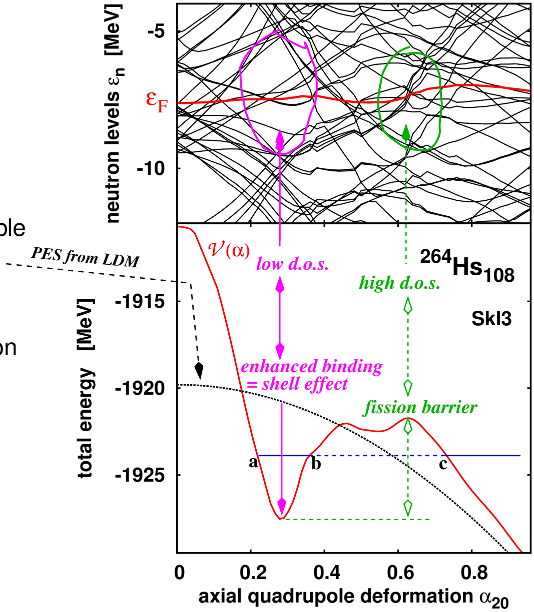

Fission properties for systematically varied Skyrme forces

exploit uncertainties in Skyrme parameterization to explore allowed variations

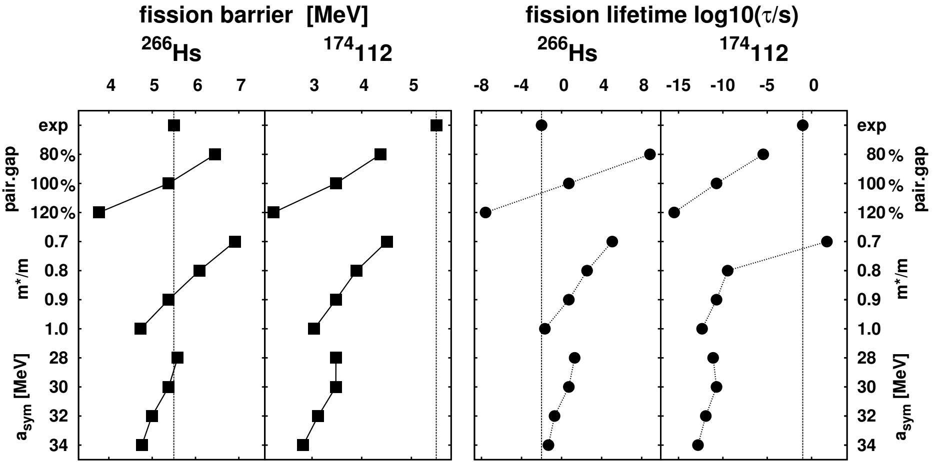

pairing has strongest effect on fission, next important is m^*/m ($\leftrightarrow$ shell struct.) and $a_{\rm sym}$

variations in ^{266}Hs and 112/174 go in parallel $\longrightarrow$ no help for too short $\tau_{\rm SF}$ in 112/174

Fission path –example ^{236}U

pure LDM ⇒ unstable
stabilized by shell effects
⇒ : subtle balance between

LDM and shell structure

m*/m *effective mass*
κ *sum rule enhanc.*
(=isovector m/m)*
*l*s models*

K *incompressibility*
a_{sym} *symmetry energy*

ZPE: lowering 0–0.5 MeV (1.barr.)
triaxiality: lowering 1. barr 0–2 MeV

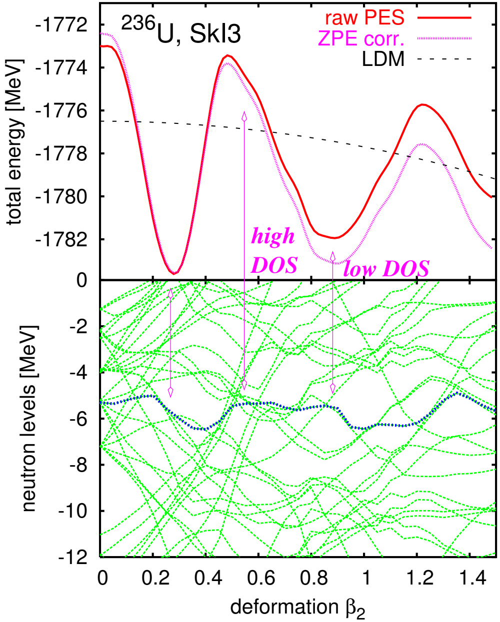

Lifetimes for neutron induced fission

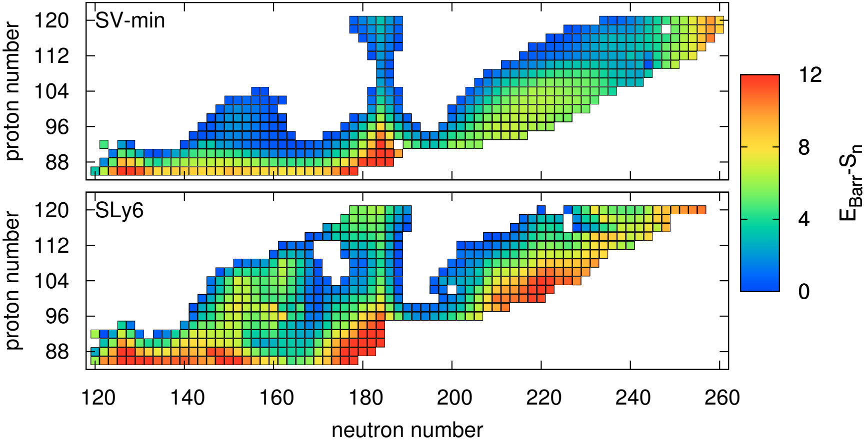

Computation of α-decay lifetimes nuclear fission

Estimate via the Viola-Seaborg relationship:

$$\log\left(\frac{\tau_\alpha}{\mathrm{s}}\right) = (a*Z+b)(Q_\alpha/MeV)^{-1/2} + (c*Z+d) + h_{\log}$$

$$a = 1.66175,\ b=-0.5166,\ c=-0.20228,\ d=-33.9069$$

Key ingredient is the Q_α value:

$$Q_\alpha = E(N-2,Z-2) - E(N,Z) + E(2,2)$$

$$E(2,2) = E_{\mathrm{exp}}(^4\mathrm{He}) = 28.3 MeV$$

$E(N,Z) \quad \longleftrightarrow \quad$ deformed mean-field calculation

Test of β-decay halflives